JOURNAL OF GEOPHYSICAL RESEARCH, VOL. 86, NO. C12, PAGES 11,995–12,014, DECEMBER 20, 1981

The Effect of a Geographical Cloud Distribution on Climate: A Numerical Experiment With an Atmospheric General Circulation Model

V. P. MELESHKO

Voeikov Main Geophysical Observatory, 194018, Leningrad, USSR

R. T. WETHERALD

Geophysical Fluid Dynamics Laboratory, NOAA, Princeton University, Princeton, New Jersey 08540

This study is an attempt to estimate the effect of a geographical distribution of clouds on climate. A method of determination of a three-dimensional cloud distribution is proposed. It is based on the solution of the inverse problem for the radiative transfer equation. By using climatic data on total cloud amount, temperature, mixing ratio of water vapor, and satellite data on outgoing longwave radiation, the global distributions of high, middle, and low clouds were computed for July. The derived vertical cloud extension is in fair agreement with available data on the frequency distribution of stratiform and cumulus clouds. Two numerical experiments are carried out with an atmospheric general circulation model in which zonal and geographical cloud distributions are prescribed. The integrations are performed for 60 days with a GFDL model, and the last 30 days are analyzed. The geographical cloud distribution causes the increase of surface temperature over the continents by 2°–4° and leads to a decrease of surface pressure there and an increase over the oceans. The largest changes in the surface pressure, up to ±12 mbar, occur in the middle latitudes of both hemispheres. The largest differences in precipitation are observed in the tropics and over some coastal regions of North and South America. Arid areas in the subtropical belt become more pronounced in case of the geographical distribution of clouds. Estimates of the level of significance for precipitation and surface pressure changes reveal that they are statistically significant in some areas of the globe.

1. INTRODUCTION

In recent years a number of studies have been performed in which cloud effects upon climate have been considered. The primary emphasis of most studies was concentrated on the problem of how will the atmosphere respond if the fractional cloud cover or their vertical extension changes as a result of a natural or anthropogenic impact on the atmosphere. A similar question arises when different cloud parameterization techniques are used in atmospheric general circulation models.

The effect of cloud amount change on surface temperature was studied with a radiative-convective model by *Manabe and Wetherald* [1967]. It was found that an increase of fractional cover of low and middle clouds decreases the surface temperature. It was also found that the effect of surface cooling decreases as cloud height increases. In particular, if high clouds are assumed to have a blackbody emissivity, their increase produces a heating of the surface.

The sensitivity of the earth-radiation balance to cloud cover change was studied by many investigators [*Schneider*, 1972; *Cess*, 1976; *Ellis*, 1978; and others]. The estimation of cloud feedback for zonally and globally averaged values of the radiation balance revealed significant differences between the results obtained by different authors. As indicated by *Cess* [1978] a large portion of these differences can be attributed to the implicit assumptions on functional dependence of cloud cover change at different heights upon the change of total cloud cover. In part they can also be associated with differences in used optical cloud parameters, prescribed cloud heights, number of cloud layers, etc. Employing zonally averaged annual climatological data for the northern hemisphere, *Cess* [1976] suggested that cloud amount change may not be a significant climate feedback mechanism.

Paper number 1C1294.

There are some studies in which regional effects of clouds on the long-term state of the atmosphere have been evaluated. They show that the cloud-radiation feedback may be pronounced over some regions of the globe and produces significant changes not only in the thermal state of the troposphere but also in the hydrological cycle of the atmosphere through modification of the general circulation.

Charney et al. [1977] studied the effect of a surface albedo change on the development of drought in the semi-arid regions and found that the cloud change can be even more significant than the surface albedo change in maintaining the surface thermal regime. As a result, the positive feedback mechanism (an increase in surface albedo causes a cooling of the low troposphere, damps upward motion and decreases the precipitation rate thus favoring the enhancement of an arid condition) could be completely canceled because the surface-cloud albedo change is larger than the surface albedo change alone.

Musaelyan [1974, 1978] analyzed observational data for a 10-year period and found a close relationship between the cloud anomalies over the North Atlantic in summer and anomalies in the thermal state of the atmosphere in Europe during winter 6 months later. In his opinion, this relationship is associated with a long-term variation of the cloud distribution. If the cloud cover is less than its mean climatic distribution over the North Atlantic in summer, the upper oceanic layer receives and accumulates a larger amount of solar energy. In winter, the atmosphere receives more heat from the ocean which favors warmer winters in Europe as compared with the mean condition. If a larger cloud amount is observed over the North Atlantic in summer, then the following winter will be cooler in Europe.

The above studies show that there is no generally accepted opinion on the size and magnitude of cloud feedback on climate. To a great extent it reflects imperfections of cloud pre-

diction schemes used in the atmospheric models and an inadequate knowledge of the sensitivity of radiative forcing to uncertainties associated with cloud prediction. At the present time there exists several different ways of including clouds in the atmospheric models: some studies were performed with prescribed cloud distributions [*Manabe et al.*, 1979], and in others the clouds were computed in terms of predicted model parameters [*Somerville et al.*, 1974; *Gates and Schlesinger*, 1977; *Washington and Williamson*, 1977; *Wetherald and Manabe*, 1980]. In most models the heights and thicknesses of the clouds are prescribed and fractional cloud cover is computed by means of empirical formulae in which the cloud amounts of specific layers are related either to relative humidity or to the occurrence of condensation. In the Wetherald-Manabe model, clouds are placed in those layers where condensation (precipitation) occurs.

The aim of the present study is to assess the sensitivity of the mean state of the atmosphere to two different methods of cloud specification in the atmospheric model. It has been mentioned that several climate studies at the Geophysical Fluid Dynamics Laboratory have been performed with a prescribed zonally averaged cloudiness at three levels.

It is of interest to determine how the regional climate might be changed if, instead of zonal clouds, their 'observed' geographical distribution is incorporated into the model. The so-called observed clouds were obtained from the solution of the simplified radiative transfer equation, by taking into account satellite data for outgoing terrestrial radiation, climatic data for temperature humidity, total cloudiness, and a radiation calculation of terrestrial fluxes. A description of the method used for the computation of cloud amount at three specified levels of the atmosphere and the results of these computations are given in the appendix.

It is worth noting that the present study is carried out under the assumption that the cloud cover does not change with time for both experiments. In other words, the effect of atmospheric processes on the cloud cover evolution is not considered. Furthermore, because the ocean surface temperature is prescribed, the feedback between clouds and surface temperature is also excluded. Owing to the large thermal inertia of the ocean, the second assumption might not be very restrictive if the response of the atmosphere is considered for the time span of about one season. This is because the large oceanic heat capacity delays or inhibits a significant interaction between the prescribed cloudiness change and the corresponding surface radiative change over the ocean during the relatively short integration period considered in this investigation. Despite these two simplifications, the results of the study are of certain interest since they may provide useful insight into an understanding of the climate sensitivity to cloud changes.

2. DESCRIPTION OF THE ATMOSPHERIC MODEL

A semi-spectral baroclinic general circulation model of the atmosphere is used in this study. The basic spectral transform theory was proposed by *Orszag* [1970] and *Eliassen et al.* [1970]. Adopting this technique, *Bourke* [1974], *Bourke et al.* [1977], *Hoskins and Simmons* [1975], and *Gordon and Stern* [1981] developed 'semi-spectral' baroclinic models of the atmosphere. The model used in the current experiments is one constructed by the Climate Dynamics Group of the Geophysical Fluid Dynamics Laboratory, by combining Gordon's spectral dynamics with a previously developed portion of the climate model in which various physical processes are incorporated [*Manabe et al.*, 1979]. A detailed description of its numerical algorithm, physical processes incorporated, and its ability to simulate the climate for January and July can be found in a number of publications [e.g., *Bourke et al.*, 1977; *Holloway et al.*, 1971; *Manabe et al.*, 1979]. Therefore, only a brief description of the model is given below.

The basic prognostic variables of the spectral model are relative vorticity, divergence, temperature, water vapor mixing ratio, and logarithm of surface pressure. The horizontal resolution of the model is described by the number of spherical harmonics incorporated. In the present study the model including 21 wave components along a latitude circle with rhomboidal truncation of waves in the meridional direction is used. Nonlinear terms of the main equations are estimated at grid points and then transformed into wave components by means of the fast Fourier transform technique. The number of equally spaced grid points along a latitude circle is 48 and 40 points are taken along meridians at so-called Gaussian latitudes. In the vertical, a σ coordinate system is used that makes it possible, in a comparatively simple way, to incorporate the topography of the continents. The vertical structure of the atmosphere is described with nine levels, which are chosen in such a way that they provide a higher resolution near the boundary layer and at the lower stratosphere. The horizontal diffusion of relative vorticity, divergence, heat, and water vapor is taken as proportional to the differential operator of the fourth order. The coefficient of proportionality is the same for all four variables.

The heat flux divergence due to terrestrial radiative transfer is computed with the same scheme that is used for estimation of the vertical cloud distribution. The method of computation of solar radiative transfer is described by *Manabe and Strickler* [1964], *Manabe and Wetherald* [1967], and *Wetherald and Manabe* [1975]. The solar radiation at the top of the atmosphere is a function of both season and latitude, but its diurnal variation is eliminated. The clouds are prescribed at three levels, and their distribution does not change with time. With regard to terrestrial radiation, the clouds are assumed to be black bodies. For solar radiation, the optical properties of the clouds are the same as those given in Table 1 of *Wetherald and Manabe* [1980]. The prescribed spatial cloud distribution depends on the type of experiment and this matter is outlined in the next section.

The processes of heat and water vapor exchange between the surface and the atmosphere and within the atmosphere itself due to turbulent transfer, convection, and condensation are described by *Manabe et al.* [1979]. A seasonal variation of surface temperature is prescribed for the oceanic regions. The temperature distribution for a particular month over the ocean is computed by means of interpolation from its monthly values given for the four seasons [*Manabe et al.*, 1979]. The temperature of the continental surface is determined such that it satisfies the requirement of heat balance among the net incoming solar radiation, the net outgoing terrestrial radiation, and the fluxes of sensible and latent heat.

3. DESIGN OF EXPERIMENTS

Two numerical experiments are conducted with the general circulation model described in the preceding section. In both experiments the mean state of the atmosphere is simulated for July, but different sets of cloud distributions are used.

The first experiment (control experiment) incorporated a zonal mean cloud cover at three model levels, whereas the sec-

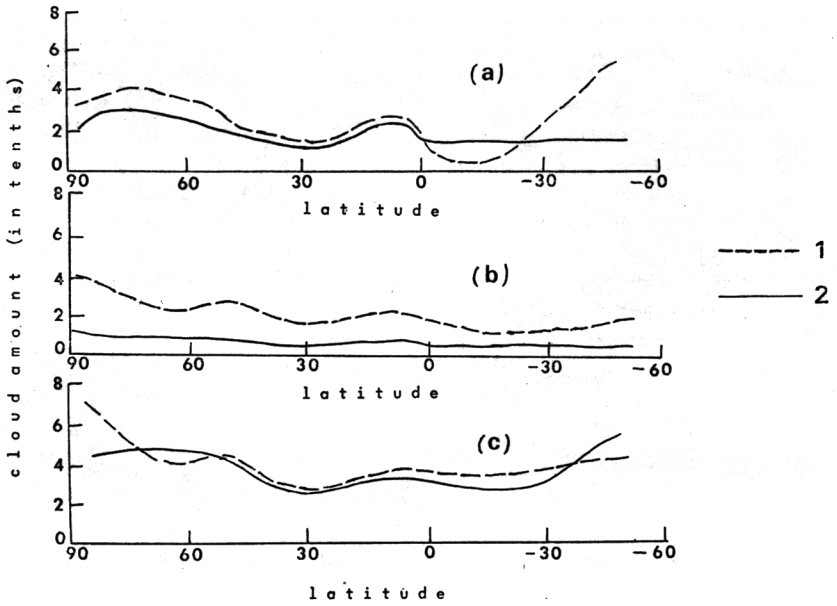

Fig. 1. Zonal distribution of (1) computed and (2) observed cloud cover of (*a*) high, (*b*) middle, and (*c*) low, clouds for July. The observed clouds at the three levels were taken from *London* [1957] and *Van Loon et al.* [1972] for the summer season.

ond experiment incorporated a geographical distribution of clouds at the same vertical levels. The zonal-mean distributions of high, middle, and low cloud cover for the control experiment are given in Figure 1, and the corresponding geographical distributions of cloud cover adopted for the second experiment are shown in Figure 2. Here, the zonal means of the geographical cloud distributions are the same as those used in the control experiment for each of the three model levels. For reference, the observed total cloud cover distribution taken from *Berlyand and Strokina* [1974] and *Van Loon et al.* [1972] is shown in Figure 3. The method of determining these separate cloud distributions consists of solving a set of simultaneous equations involving observed global distributions of total cloud cover, outgoing radiative flux, temperature, and water vapor at three levels of the model atmosphere. The three cloud levels chosen for this study are the same as those given by *Feigelson* [1970] and *London* [1957]. For a detailed description of the method of cloud derivation for the three separate levels, the reader is referred to the appendix.

It is important to note here that in both experiments the cloudiness used is consistent with both the total cloud amount and terrestrial radiation at the top of the atmosphere (with some exception for high latitudes of the southern hemisphere). For convenience of further discussion, we shall refer to the experiment with zonal cloudiness as ZCL and the experiment with geographical cloudiness as GCL.

The model is integrated from an initial state, which corresponds to the date of June 1, for 2 months, i.e., until August 1. The results of another long-term simulation are used as an initial state of the atmosphere for the experiments. The simulated atmosphere is analyzed for the last 31 days of integration which are considered as relevant to the July state.

Figure 4 represents the geographical distribution of the differences in total cloud cover between the two experiments (GCL-ZCL). The shaded areas indicate the regions where the cloud cover is larger in the ZCL experiment as compared to the GCL experiment. This figure gives some indication of the probable variation of the radiative forcing in the model atmosphere that is expected to produce differences in the mean state of the atmosphere. It may be noted that a substantial spacial variation of the cloud differences takes place in the northern hemisphere, where the larger differences in the properties of ocean and land surfaces occur as compared to the southern hemisphere. For example, the rms deviation of cloud cover from its zonal distribution is 0.17 in the northern hemisphere and less than 0.13 in the southern hemisphere. Cloud cover over the continents is found to be smaller in the GCL experiment (negative anomaly) than in the ZCL experiment. Extensive areas of negative cloud anomalies are located over North and South Africa, Arabia, Central Asia, Australia, and the western coast of North America. The areas of southeast and fareast Asia where positive cloud anomalies occur are exceptions to the above. A considerable cloud cover is formed there in connection with the development of the southwest and southeast monsoons at that time of the year. Other regions with positive cloud anomalies are observed in equatorial Africa and Central America, and their existence is associated with the location of the intertropical convergence zone over the continents. A generally opposite picture can be found over the oceans, where positive anomalies of total clouds occur.

Figure 5 shows the geographical distribution of differences in high, middle, and low clouds between the two experiments (GCL-ZCL). This figure contains some additional interesting features relevant to the differences in the vertical extent of the clouds. For example, the increase of total cloud cover illustrated in Figure 4 over southeastern Asia appears to be attributable to an increase of high cloud cover (Figure 5*a*), whereas the large negative anomalies over the continents are mainly due to decreases of low cloud cover (Figure 5*c*). Also, the large positive anomalies of total cloud cover over the North Pacific, North Atlantic, and off the west coast of South America are caused primarily by increases of low cloud cover over these regions. In general, changes of middle clouds (Figure 5*b*) do not contribute significantly to the overall change in total cloud cover.

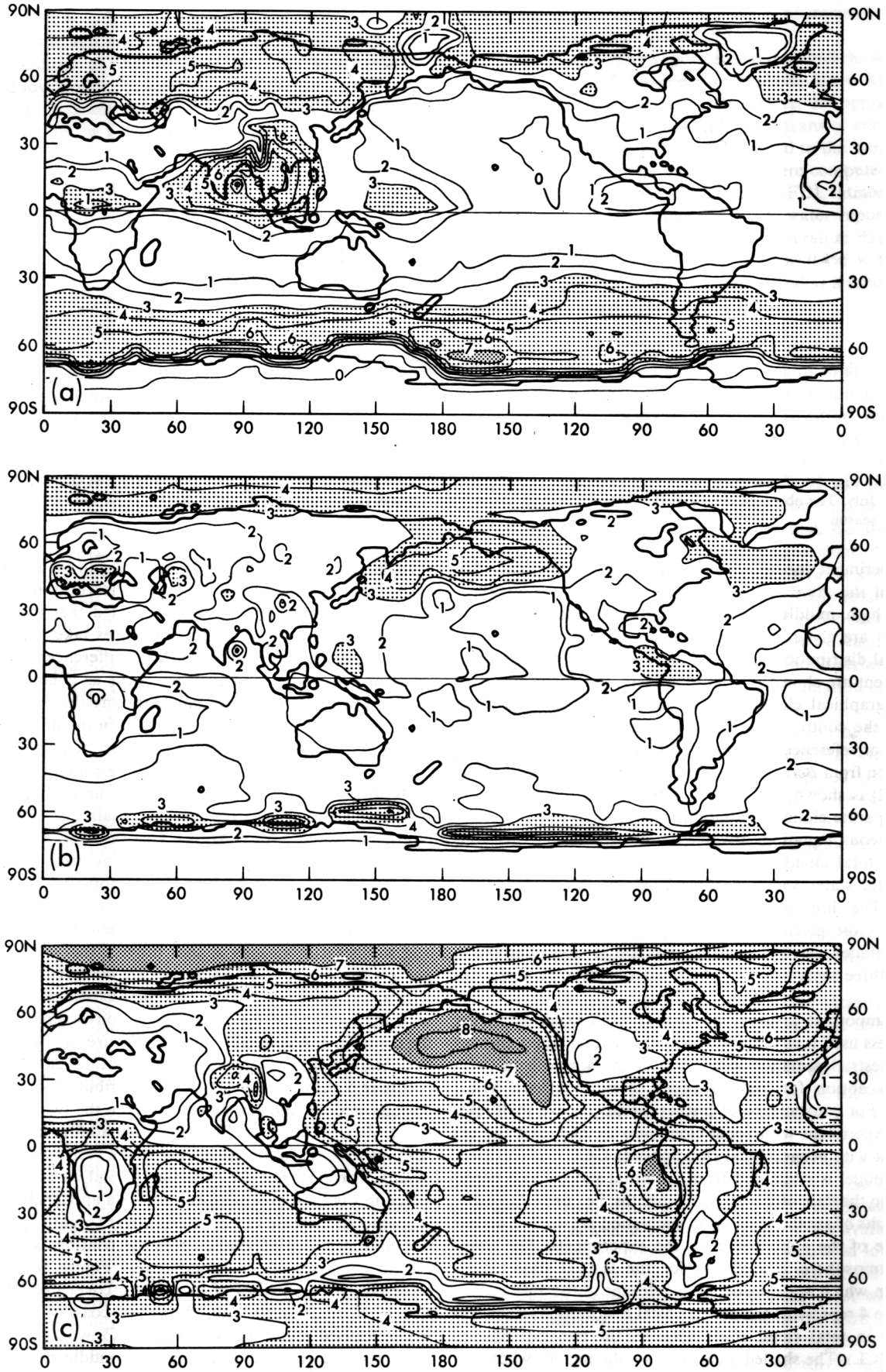

Fig. 2. Geographical distribution of computed (*a*) high, (*b*) middle, and (*c*) low cloud cover (in tenths) used for the second experiment.

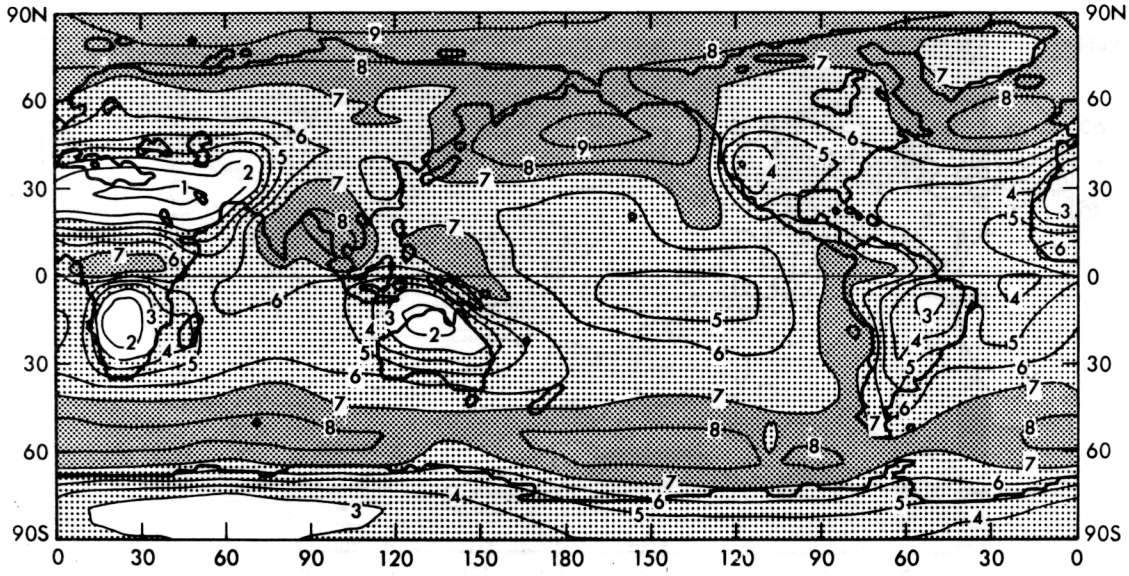

Fig. 3. Geographical distribution of observed total cloud cover (in tenths) for July [*Berlyand and Strokina*, 1974; *Van Loon et al.*, 1972].

Now, an attempt will be made to identify the differences in the state of the atmosphere produced by the cloud anomalies and to determine how significant they are.

4. Earth-Atmosphere Radiation Balance

The radiation balance of the earth-atmosphere system is an algebraic sum of the fluxes for solar radiation coming down to the top of the atmosphere, diffusive and reflected radiation to space by the atmosphere, and the earth surface and long wave emission to space by the earth-atmosphere system. The net flux at the top of the atmosphere represents gain, if it is positive, or loss of heat energy per unit area by the system.

Table 1 contains mean hemispheric values of the total radiation balance of the earth-atmosphere system as computed from the experiments ZCL and GCL. It is worth noting that the total radiation balance changes by about 8% in the northern hemisphere for the experiment GCL, and this is associated only with the spatial cloud cover differences since the hemispheric total cloud cover is the same for both experiments. On the other hand, the radiation balance changes very little for the southern hemisphere, and that is, qualitatively, in agreement with a smaller spatial variation of the total cloud cover between the ZCL and GCL experiments.

Figures 6*a* and 6*b* show the geographical distribution of the radiation balance of the system computed from the experiments ZCL and GCL, respectively. In the case of zonal cloudiness, the net flux reveals its well-pronounced zonal distribution. Some deviation from zonality in the northern hemisphere can be attributed to the differences of the albedo and temperature between the continents and oceans. On the other hand, an incorporation of a geographical cloud distribution produces a noticeable deviation from zonality in both hemispheres. Particularly marked variations are evident in the northern hemisphere.

The geographical distribution of differences in the net radiation flux between the two experiments (GCL-ZCL) is given

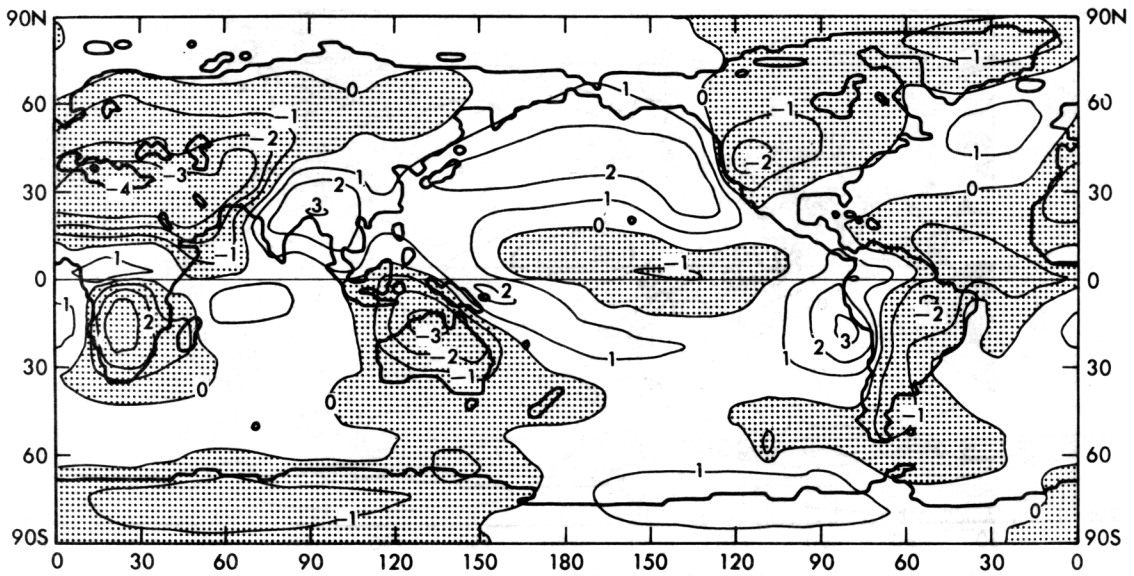

Fig. 4. Deviation of total cloud cover (in tenths) from its zonally averaged distribution.

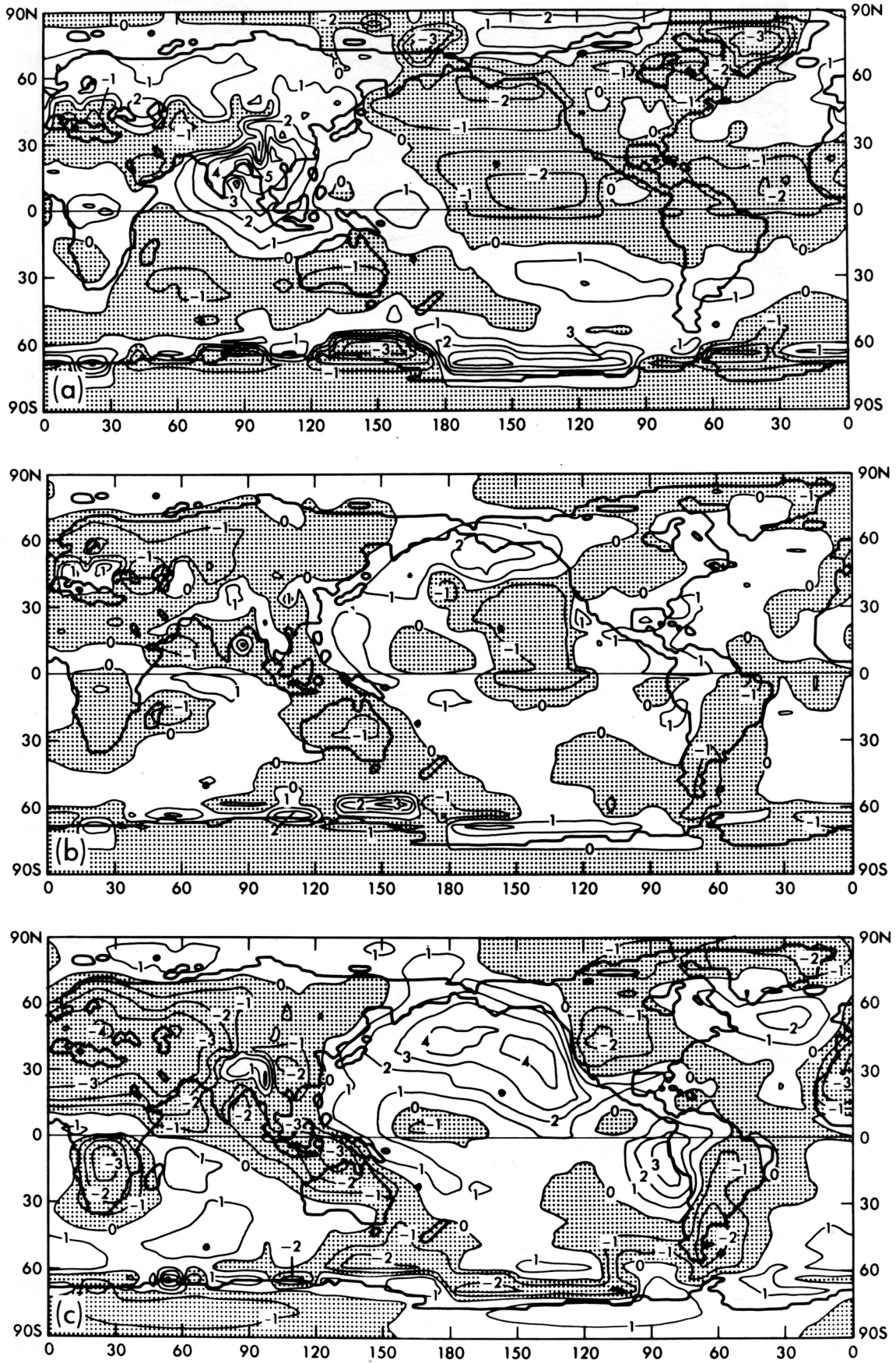

Fig. 5. Deviations of (*a*) high, (*b*) middle, and (*c*) low, cloud cover (in tenths) from their zonally averaged distributions.

TABLE 1. The Mean Hemispheric Values of the Total Radiation Balance of the Earth-Atmosphere System (in W/m^2) and Total Cloud Cover in the Experiments ZCL and GCL

Experiments	Northern Hemisphere		Southern Hemisphere	
	Radiation Balance	Total Cloud Cover	Radiation Balance	Total Cloud Cover
ZCL	53.7	0.61	−78.8	0.58
GCL	49.5	0.61	−79.5	0.58

in Figure 7. The geographical cloud distribution produces a variation in the radiation balance of ±70 W/m^2 and that amounts to 50% of its variation between the tropics and high latitudes for the winter hemisphere. The figure shows some gain of heat energy by the earth-atmosphere system over the continents. Comparison of these differences with differences for total cloud amount (Figure 4) reveals that the gain of energy is generally attributed to the reduction of planetary albedo over the continents caused by the decrease in total cloudiness. A similar relation holds over North and South Africa, North America, Europe, and most of Asia. However, there are areas where this close correlation is violated. For example, a heat gain is also observed over southeast Asia with a distinctive positive anomaly of the total cloudiness. Moreover, it extends toward northern Australia where the area with minimum total cloud cover is positioned only over the continent in the GCL experiment. To understand this it is worth considering in more detail the vertical structure of the clouds over the area concerned and their radiative properties (see Figures 5*a*, 5*b*, and 5*c*).

As follows from Figures 5 and 7, the positive change of the earth-atmosphere radiation balance over India and southeast Asia correlates well with some reduction of middle and, particularly, low clouds in the region. This implies that the warming of the earth-atmosphere system is most likely defined by the vertical change in cloud cover than by the increase in total

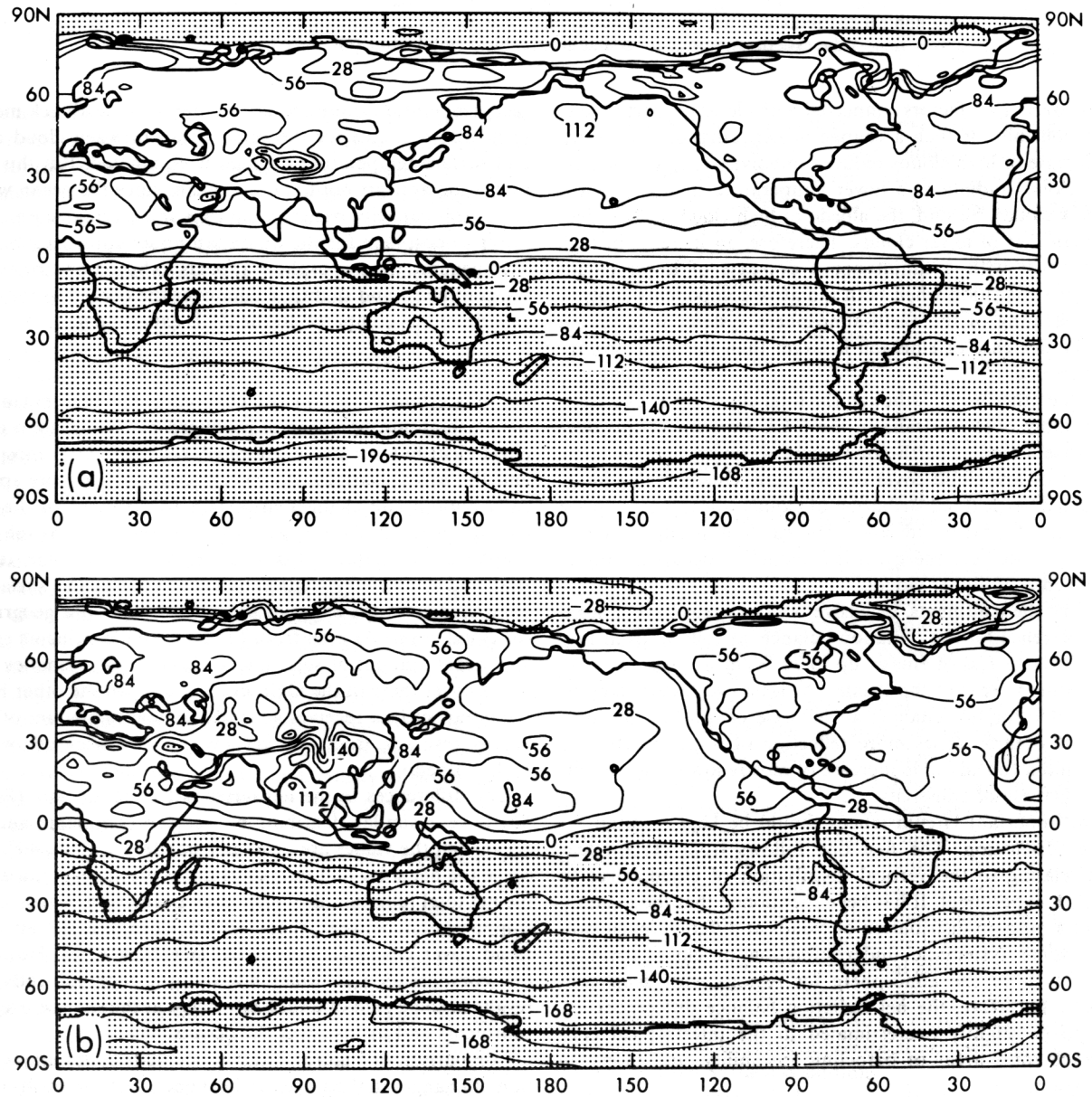

Fig. 6. Geographical distributions of net radiation flux at the top of the atmosphere (in w/m^2) computed in the experiments with (*a*) zonally averaged and (*b*) geographical cloud cover.

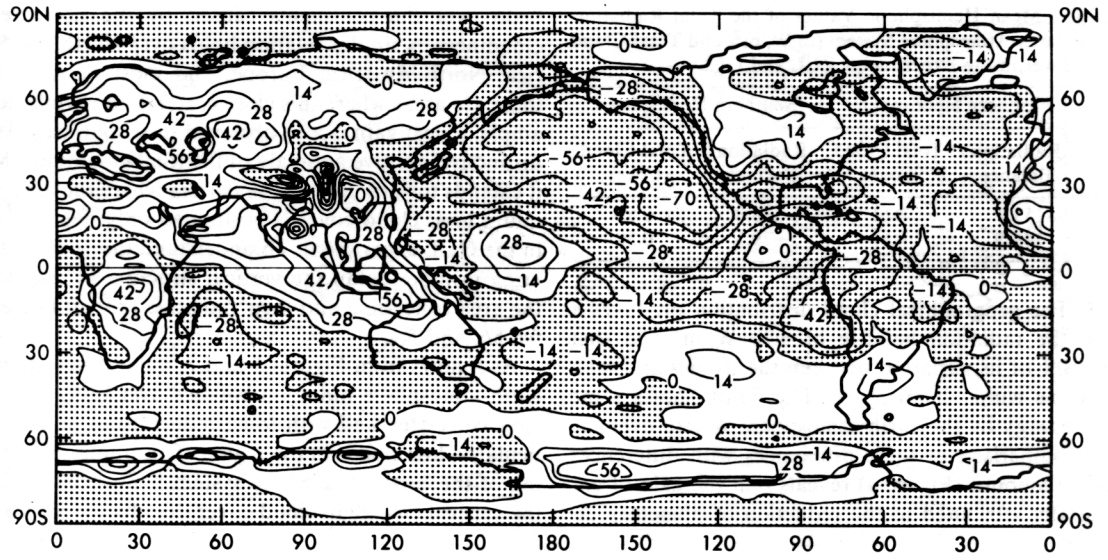

Fig. 7. Geographical distribution of net radiation flux difference at the top of the atmosphere (in w/m^2) computed from the experiments with zonal and geographical cloud cover (GCL-ZCL).

cloud cover. Two factors connected with cloud properties may be responsible for such a change of net radiation flux. First, an increase of high clouds reduces emissivity to space because these clouds radiate at a lower temperature than do middle and low clouds. Second, the albedo of high clouds is 2–3 times less than that of lower clouds. Therefore, an increase in high cloud cover with a simultaneous decrease of lower clouds leads to a condition when both radiative components contribute to heating of the earth-atmosphere system. It turns out that the decrease of emission is larger than the solar absorption increase.

On the other hand, although the total cloud cover decreases appreciably over Australia in the GCL experiment this does not cause a similar earth-atmosphere warming because some increase of low cloud cover occurs there. One can also imagine such a vertical redistribution of clouds when, despite some reduction of total cloud cover, the earth-atmosphere system may even lose heat energy, if this reduction occurs mainly at the expense of higher clouds.

Unlike the continents, extensive oceanic areas have a negative difference for the radiation balance, as follows from Figure 7. A large loss of energy up to 70 W/m^2 is observed over the northern areas of the Pacific. At least two factors may be responsible for this change: an increase of total cloud cover over the oceans causes more reflection of solar radiation to space and a considerable increase of mostly low clouds results in an increase of emissivity.

Two important circumstances should be kept in mind for further discussion. The first one follows from certain features relating to the vertical distribution of cloud cover in the GCL experiment. It has been mentioned that the assumption of a random distribution of clouds at different levels produces some systematic underestimation of cloud cover at lower levels of the atmosphere for regions with deep convection. Therefore, the net radiation balance differences appear to be slightly overestimated in the intertropical convergence zone, areas of baroclinic instability, and monsoon circulation.

The second point concerns the sensitivity of the atmosphere to changes of cloud cover over the oceans. Since the sea-surface temperature is prescribed, an important feedback mechanism that accounts for the relationship between cloud cover and surface temperature changes is eliminated. But this simplification appears not to be significant since the ocean with a large heat capacity basically controls the thermal state of the lower troposphere for the time span under consideration.

In general, the troposphere appears to become warmer over the continents and slightly colder over the oceans in the GCL experiment as compared to the ZCL experiment.

5. Heat Balance of the Surface

To ascertain as to how the changes in the heat balance of the earth-atmosphere system produced by the different cloud cover distributions are partitioned between the atmosphere and the earth's surface, it is worth considering more specifically appropriate changes in certain components of the heat balance at the surface. Figures 8*a*, 8*b*, and 8*c* show the geographical distribution of differences of the net solar, terrestrial, and total (net) radiation balance at the earth's surface as computed from the experiments with a zonal and geographical cloud cover. As seen from Figure 8*a* the continents gain a significant amount of solar energy because of a smaller total cloud cover there in the GCL experiment. On the other hand, the ocean surface receives generally a smaller amount of heat energy resulting from a larger amount of low clouds with a higher albedo.

The differences in the net terrestrial radiation flux (Figure 8*b*) have a similar distribution over the continents and the oceans but the values are generally smaller by about 40%. Because the net solar and terrestrial fluxes are incorporated into the net total radiation flux with an opposite sign, a substantial compensation between them occurs when the net effect of cloud cover change is considered (see Figure 8*c*). However, this compensation is rather nonuniform geographically and results in some gain of total heat energy at the surface over the continents and its loss over the oceans.

Comparison of Figures 7 and 8*c* shows that the major portion of changes in the radiative heat energy of the earth-atmosphere system is associated with its respective changes of the same sign at the surface. However, there are some exceptions.

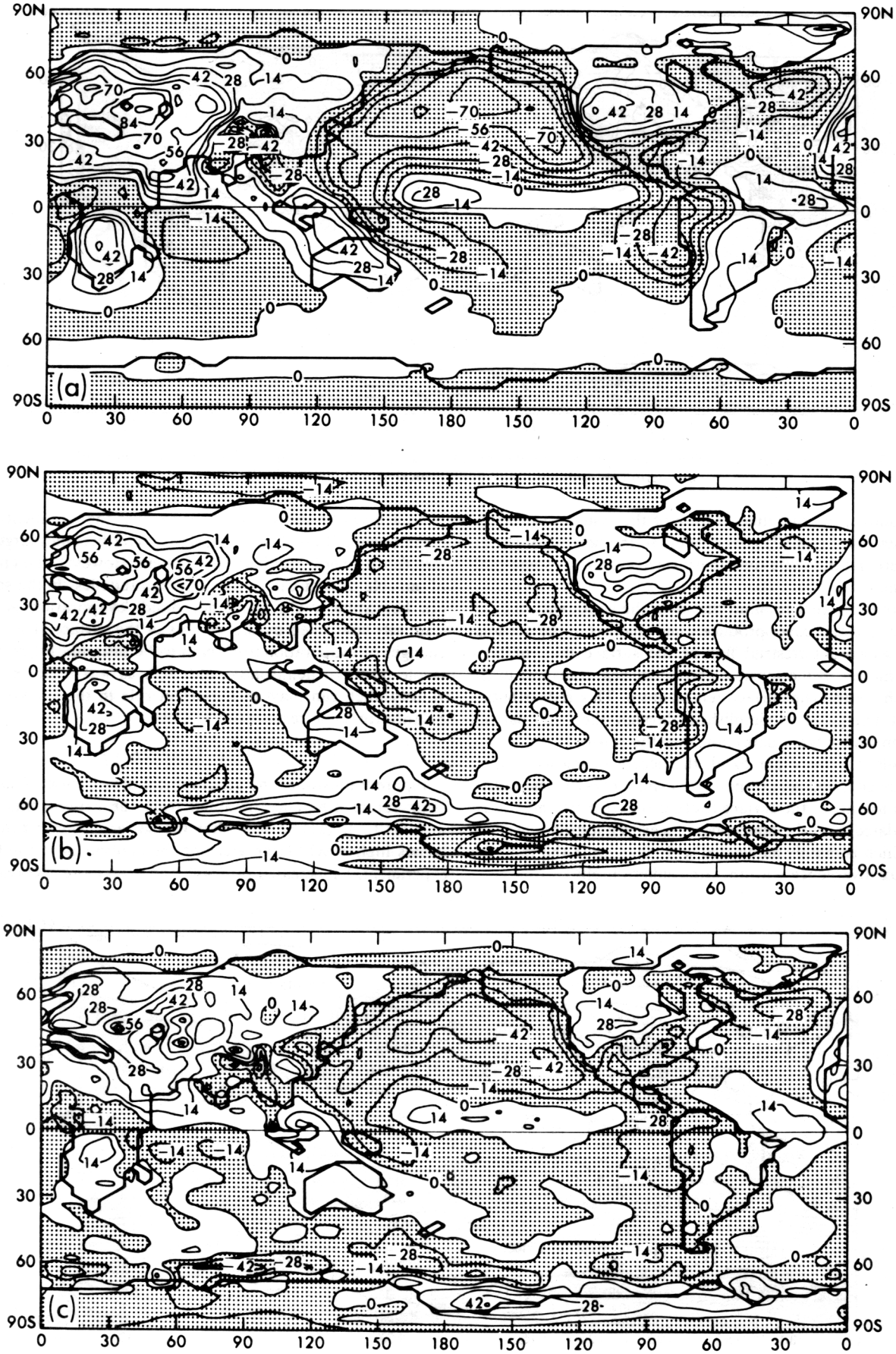

Fig. 8. Geographical distributions of differences for (*a*) net solar, (*b*) terrestrial, and (*c*) total radiation balance of the surface (in w/m^2) computed from the experiments with zonal and geographical cloud cover (GCL-ZCL).

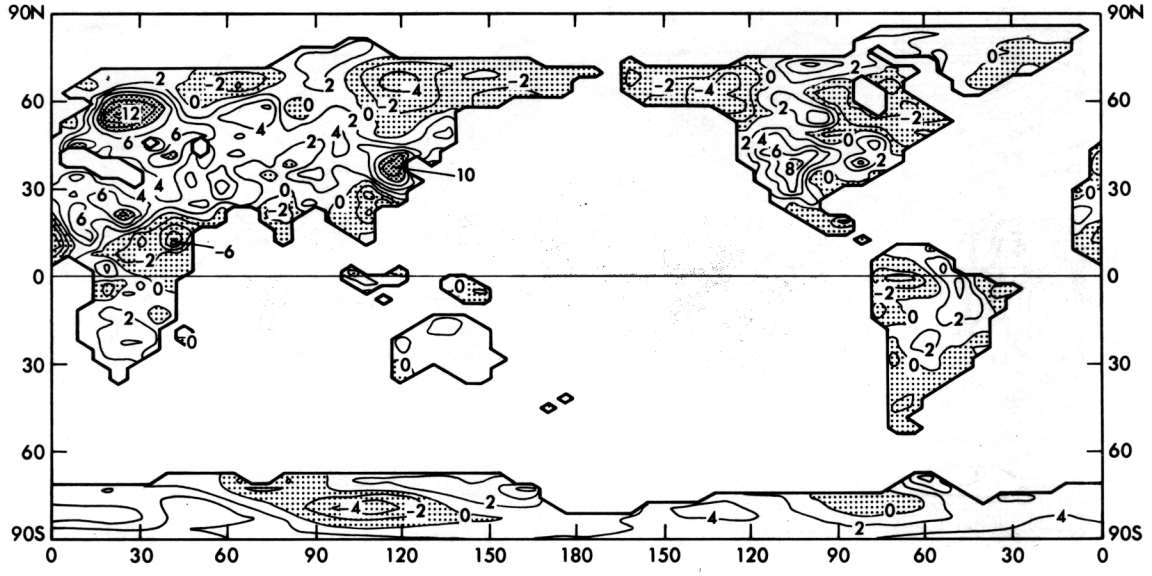

Fig. 9. Geographical distribution of surface temperature differences over continents (in degree Celcius), computed from the experiments with zonal and geographical cloud cover (GCL-ZCL).

For example, the radiative heating of the system over southeast Asia (see Figure 7) goes entirely to the heating of the atmosphere. At the same time the surface even loses some radiative energy.

It should be kept in mind that over the continents, the differences in cloud cover produce some changes in the net solar and downward terrestrial flux at the surface that, in turn, cause changes in the sensible and latent heat transport to the atmosphere and the surface temperature. This redistribution of heat energy is accomplished through the heat balance equation under the assumption that the soil heat capacity is negligible. On the other hand, the ocean, owing to its large heat capacity, does not respond in a similar way to the radiative flux forcing at the surface (even if the surface temperature is calculated) and the atmosphere receives additional heat energy which is mainly associated with changes in the radiative heat flux divergence with the atmosphere itself.

As a result of the surface heating over the continents, the mean sensible heat flux to the atmosphere becomes larger by 20% for the whole northern hemisphere. However, the change of sensible heat flux is 1 order of magnitude less in the southern hemisphere. On the other hand, evaporation is substantially controlled by the wetness of the surface. The mean changes of evaporation are found to be insignificant over the whole northern hemisphere, although as was indicated previously, they can play an important role in the surface heat balance for some regions of the globe.

6. SURFACE TEMPERATURE

Figure 9 illustrates the geographical distribution of surface temperature difference obtained from the experiments ZCL and GCL. It can be seen that the surface temperature becomes higher over large areas of the continents in the GCL experiment. Its increased by 2°–4° and even more is connected

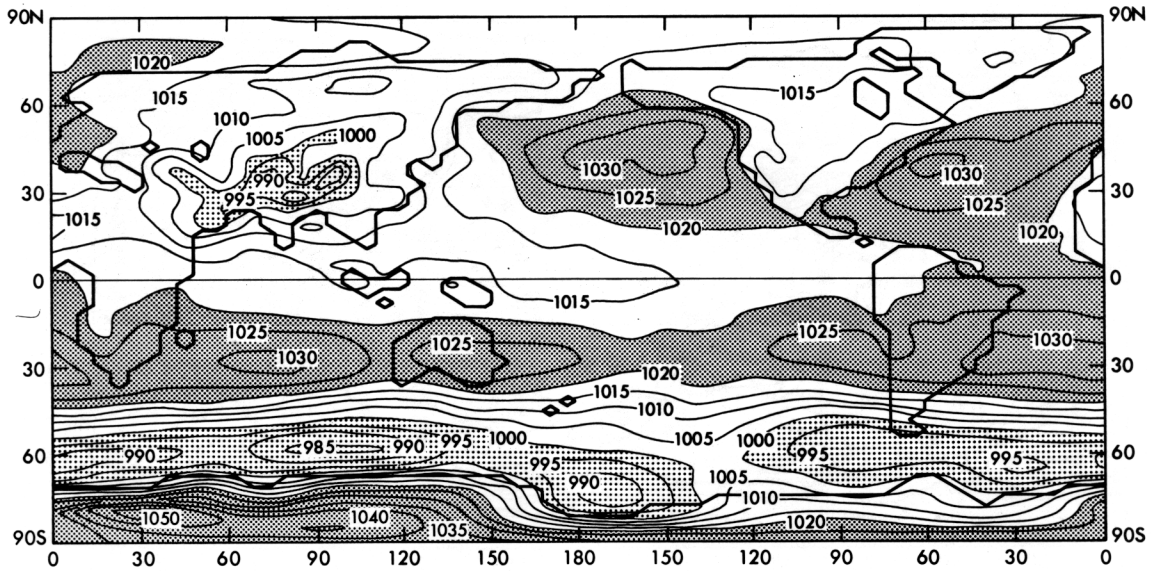

Fig. 10. Geographical distribution of sea-surface pressure (in millibars), computed from the experiment with zonal cloud cover.

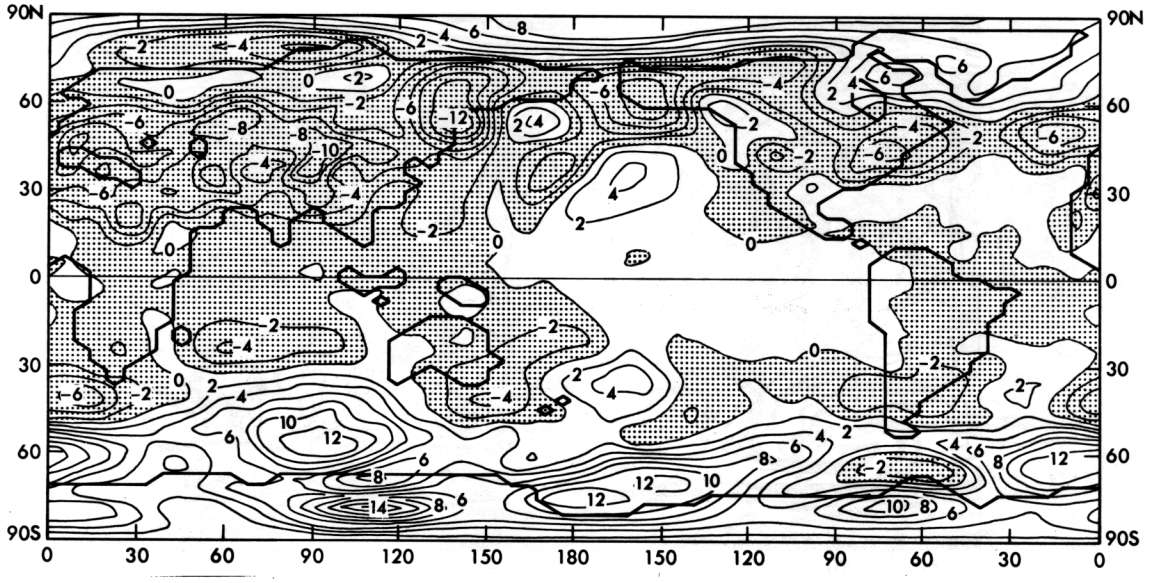

Fig. 11. Geographical distribution of sea-surface pressure differences (in millibars) computed from the experiments with zonal and geographical cloud cover (GCL-ZCL).

with a total cloud decrease over extensive areas of Asia, Europe, Africa, and North and South America. On the other hand, temperature decreases of the same magnitude occur in eastern Siberia, coastal regions of North and South America, southeast Asia, and equatorial Africa, where an increase of total cloud cover is observed. In general, this relationship between surface temperature and total cloud cover change is well illustrated over most areas concerned. However, the temperature decrease in southeast Asia has some distinctive features that seem to be worth discussing in some detail. As indicated in the previous section, a substantial increase of high cloud cover by 40–50% over the area resulted in some reduction of the net solar flux at the surface that is larger than the reduction in the net terrestrial flux in the GCL experiment as compared with the ZCL experiment. Furthermore, an analysis of the water balance component at the surface shows that the temperature decrease may also be attributed to an increase of evaporation that appears to be more efficient in the transport of heat from the surface to the atmosphere in the tropics. In turn, the larger evaporation is stipulated by an increase in precipitation and wetness of the surface. This subject will be discussed further in section 8.

7. Surface Pressure and Circulation

It is known that low pressure systems are formed over relatively warm continents of the northern hemisphere in July, and high pressure systems are formed over the oceans. Figure 10 shows the geographical distribution of surface pressure computed in the experiment ZCL. As was indicated in the preceding section, the decrease in total cloud cover over the continents causes the surface and lower troposphere to be warmer there in the GCL experiment as compared with the ZCL experiment. This causes a further decrease in the surface pressure over most parts of the continents.

Figure 11 illustrates the geographical distribution of surface pressure differences obtained from the two experiments (GCL-ZCL). The largest pressure changes, amounting to ±12 mbar, are observed in the middle latitudes of both hemispheres. The surface pressure increases over the oceans, especially in the North Pacific and North Atlantic. The intensification of high pressure systems over the oceans is likely caused by mechanisms of a dynamical nature rather than induced by thermal factors. In other words, the surface pressure increase results mainly from a mass redistribution owing to the surface pressure decrease over warmer continents. As was indicated previously, the oceanic surface temperature is prescribed, and, therefore, the cooling of the lower troposphere there owing to a larger cloud cover, for example, in the North Pacific in the GCL experiment, must be strongly reduced.

This is also confirmed by one more experiment in which the middle and low cloudiness was inadvertently excluded in the North Pacific. In spite of this change, a similar increase in surface pressure was, again, observed in the region concerned. A considerable increase of surface pressure in the middle latitudes of the southern hemisphere appears to be mostly associated with a displacement of air masses from the continents of the northern hemisphere toward the southern oceans.

The changes in the thermal regime of the continents produce corresponding changes in the mean flow. Figures 12*a* and 12*b* show the wind vector differences (GCL-ZCL) for both the surface and 830 mbar, respectively. Substantial changes in the flow are observed in the middle latitudes of the northern and southern hemispheres and that is in agreement with the larger changes in surface pressure there.

The distributions of the wind vector differences have a complicated structure in the middle latitudes, and their interpretation is not so simple in some cases because of the Coriolis forcing on the horizontal flow. However, one can determine that if the pressure differences have a properly defined low pressure pattern (see Figure 11), the differences in the wind vector distribution will show a corresponding cyclonic circulation of flow with its convergence at the center of the pattern. On the other hand, if the pressure differences show a high pressure pattern, the wind vector differences correspond to an anticyclonic circulation with divergence of the surface flow.

The new eddy circulation patterns, developed for the GCL experiment, are observed not only for the surface flow, but also at higher levels of the troposphere along the east coast of Asia and the west coast of North and South America. Incorporation of a geographically distributed cloudiness leads to a

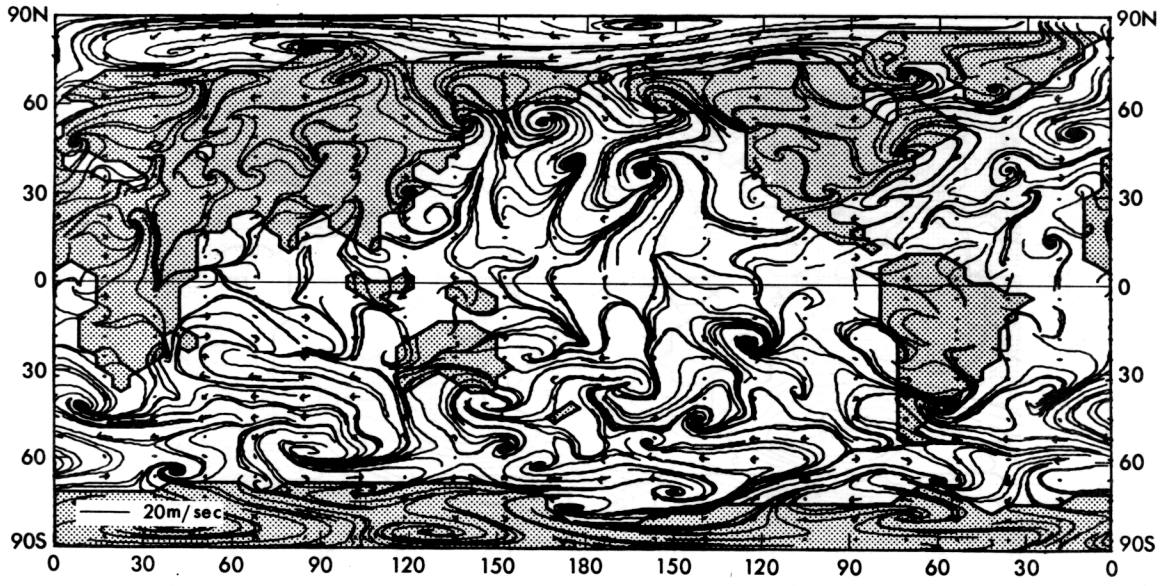

Fig. 12*a*. Geographical distribution of surface wind vector differences, computed from the experiments with zonal and geographical cloud cover (GCL-ZCL).

growth of the eddy component of kinetic energy by 12% in the northern hemisphere and its slight decrease in the southern hemisphere. It will be shown in the next section that the position and intensity of the newly formed large-scale eddies play an important role in the variation of the precipitation rate enhancing or weakening the monsoon type of circulation along the coastal regions of the continents.

8. PRECIPITATION AND LAND HYDROLOGY

Figure 13 illustrates the geographical distribution of the precipitation rate, as computed in the ZCL experiment. Characteristic features of the precipitation distribution are pronounced maxima in the intertropical convergence zone, which is positioned approximately at 5°–10°N in July; an extensive area of large precipitation rate in southeast Asia associated with the development of southwest and southeast monsoons; and areas of intensive precipitation at the middle latitudes of both hemispheres related to cyclonic activity of the atmosphere.

Figure 14*a* shows the geographical distribution of the differences of precipitation rates between the two experiments (GCL-ZCL). In spite of a rather mixed picture of their variation, interesting features are revealed over certain geographical locations. The largest changes in precipitation rate are observed in the intertropical convergence zone over the Pacific Ocean, along southeastern and eastern coasts of Asia, and North and South America. The precipitation rate variations amount to 0.5–1.0 cm/day in these regions and that corresponds to 30–50% of their total magnitude in the ZCL experiment. The intensity variations turn out to be smaller in other regions of the globe but they may be still substantial with respect to their background values.

A drastic change in precipitation rate is observed over the monsoon area (i.e., its increase over the continent and a sharp

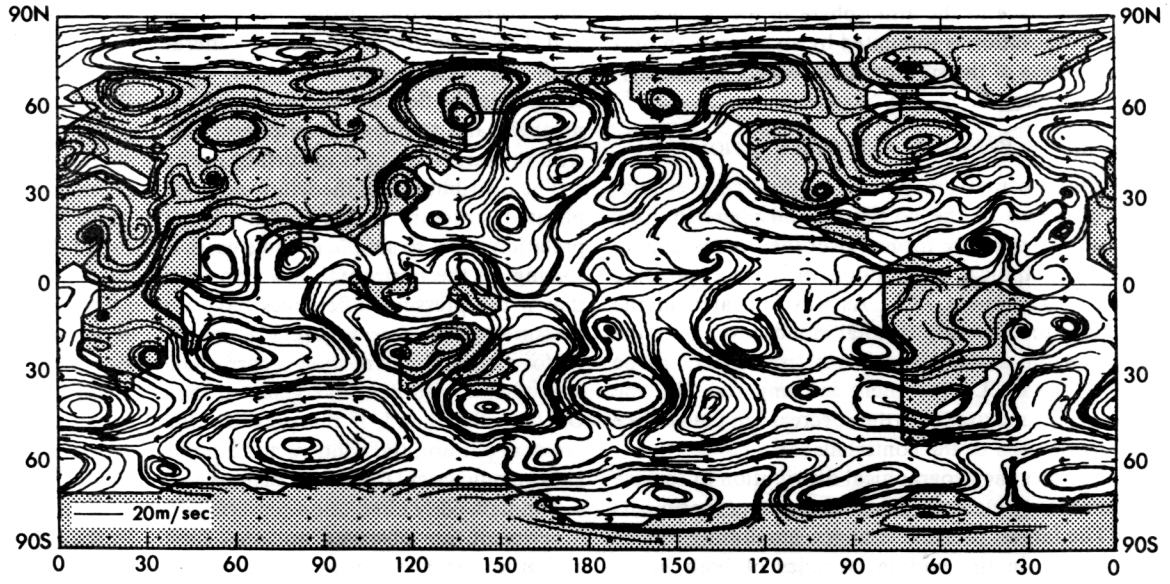

Fig. 12*b*. Geographical distribution of wind vector difference at 830 mbar, computed from the experiments with zonal and geographical cloud cover (GCL-ZCL).

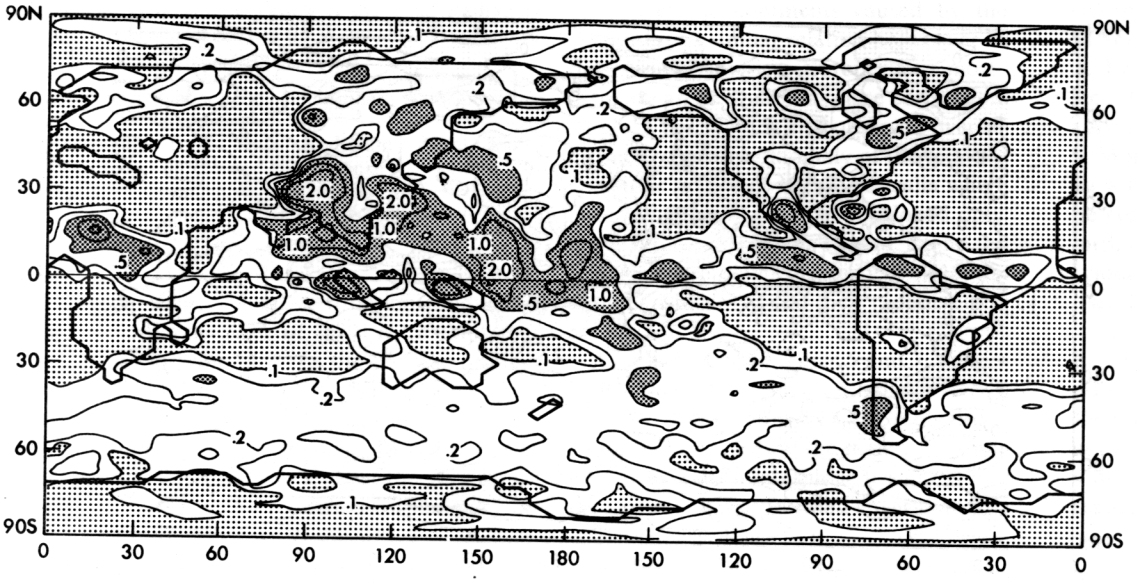

Fig. 13. Geographical distribution of precipitation rate (in cm/day) computed from the experiment with zonal cloud cover.

decrease over the Indian and Pacific Oceans adjacent to the continent). A considerable increase of precipitation over the Indochina continent is apparently caused by the intensification of a monsoon type circulation and larger transport of humid air from the ocean to the continent (see Figure 12*a*). This, in turn, is the result of the warming of air over the continent. This additional flow towards the continent is also well defined at the 830 mbar surface (see Figure 12*b*). A detailed discussion of the relationship among surface temperature, hydrology, and the monsoon circulation is given in *Webster and Chou* [1980].

It can also be seen from Figure 14*a* that precipitation decreases appreciably in the United States, North Africa, over vast areas of China, and the far east of USSR. On the other hand, a precipitation increase is observed in East Siberia next to the sea of Okhotsk, South Alaska, east and west coasts of Canada, and in southern regions of Chile and Argentina. Independent of latitude and the climatic regime of the regions concerned, the largest variation of precipitation usually takes place along the coastal area of the Asian and American continents. From comparison of Figures 12*a* and 12*b* and Figure 14*a* one can notice that the sign of the precipitation change is surprisingly well correlated with the direction of the surface wind vector difference. In other words, precipitation increases if the surface flow is directed from the ocean to the continent, and vice versa. This implies that the intensity of precipitation is mostly controlled by the monsoon-type mechanism along the coasts of the continents.

Since the ocean temperature is assigned, the response of the model atmosphere to the variation of cloudiness may be different from that of the real atmosphere over the oceans. Therefore, as noted before, the interpretation of precipitation changes there in the GCL experiment should take into account this specific feature of the model atmosphere.

Meanwhile it is of certain interest to understand the mechanisms controlling precipitation changes over the ocean, (for example, the development of small-scale patterns over a relatively uniform ocean surface in the tropical Pacific). The probable explanation of this phenomenon may be as follows. Because the net radiation flux for the surface-atmosphere system decreases due to a large cloud cover over the ocean in the GCL experiment, the troposphere undergoes some cooling. On the other hand, the oceanic surface temperature does not depend on the surface heat balance, and this contributes to a development of a more unstable condition in the lower troposphere and a larger vertical transport of moisture and condensation. An enhancement of upward vertical motion due to condensation processes must create downward motion in adjacent regions to satisfy the mass conservation requirement. The downward motion forcing may favor the weakening of condensation and precipitation rates, in some areas, thus resulting in a more patchy precipitation difference distribution.

It was mentioned near the end of section 6 that the decrease of surface temperature for the (GCL-ZCL) experiments in the monsoon region of Southeast Asia was related to an increase of wetness and evaporation there. Figure 14*b* which shows the evaporation difference between the two experiments indicates that, indeed, there is an increase of evaporation and, therefore, latent heat in this region. As was stated previously, the increased latent heating implies a more efficient transport of heat from the surface to the atmosphere, thereby reducing the surface temperature.

Figure 15*a* shows the geographical distribution of the soil moisture content over the continents in the ZCL experiment. Figure 15*b* shows the difference of soil moisture for the (GCL-ZCL) experiments. Comparison of these figures indicates that in the case of incorporation of the geographical cloud distribution, the regions with negligible moisture content, corresponding to arid and semi-arid conditions, become more extensive. Because of the higher surface temperature, sensible heat flux and evaporation to the atmosphere are increased. The warming of the lower troposphere leads to a reduction of relative humidity over the continental areas situated far away from the coast where the effect of horizontal transport of water vapor is not so significant. Some increase in evaporation without a similar increase in precipitation results in the development of drier surface conditions.

Thus, a reduction of cloud cover in the subtropical zone and some regions of middle latitudes remote from the ocean contributes to a development of drier climatic conditions over

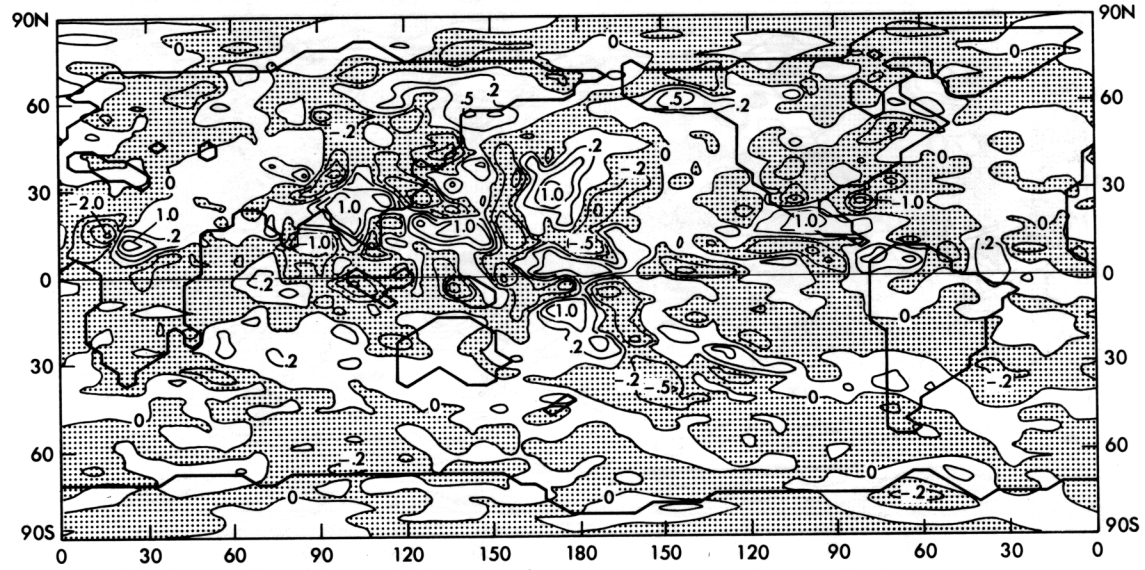

Fig. 14*a*. Geographical distribution of precipitation rate differences (in cm/day) computed from experiments with zonal and geographical cloud cover (GCL-ZCL).

the continents. On the other hand, one can note the increased wetness in the southeast Asian monsoon area caused by an enhanced hydrologic cycle there.

9. Estimation of Signal to Noise Ratio

When studying the external forcing on the atmosphere, the question arises as to whether the differences in two comparable mean states of the atmosphere are statistically significant. With regard to the present study, the prescribed cloudiness may be considered as an external forcing parameter while it is certainly an internal one for the real atmosphere.

According to *Leith* [1973] the statistical significance of differences between two states of the atmosphere is evaluated in terms of a signal to noise ratio for some considered parameter. The signal is the difference between two comparable mean states of the atmosphere. The noise defines the rms variation of the mean value when its estimation is made from a limited time series sampling. The mean change of some variable is considered as significant if the absolute value of the ratio appears to be larger than unity.

By making use of appropriate formulas for the computation of the signal and noise, proposed by *Leith* [1973], we estimated the statistical significance of changes for precipitation and surface pressure in the GCL experiment with respect to the ZCL experiment. The signal for precipitation is computed as the difference between the two mean distributions (GCL-ZCL) for the last 40 days of integration. When computing the noise distribution, the temporal autocorrelation function is zeroed out after 15 days. To eliminate some mesoscale spacial variation in precipitation, the daily values are smoothed.

Figure 16 shows the geographical distribution of the signal-to-noise ratio for the precipitation rate. Shaded areas mean that the absolute values of the ratio are equal to or greater than unity. It can be seen that almost all substantial changes, discussed in the previous section, appear to be statistically sig-

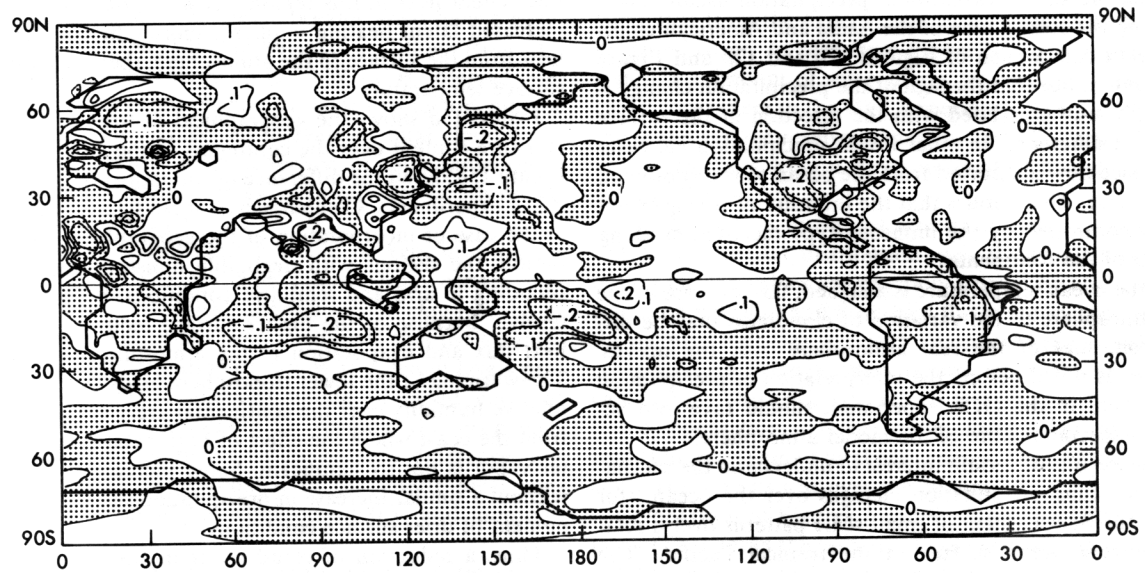

Fig. 14*b*. Geographical distribution of evaporation rate difference (in cm/day) computed from the experiments with zonal and geographical cloud cover (GCL-ZCL).

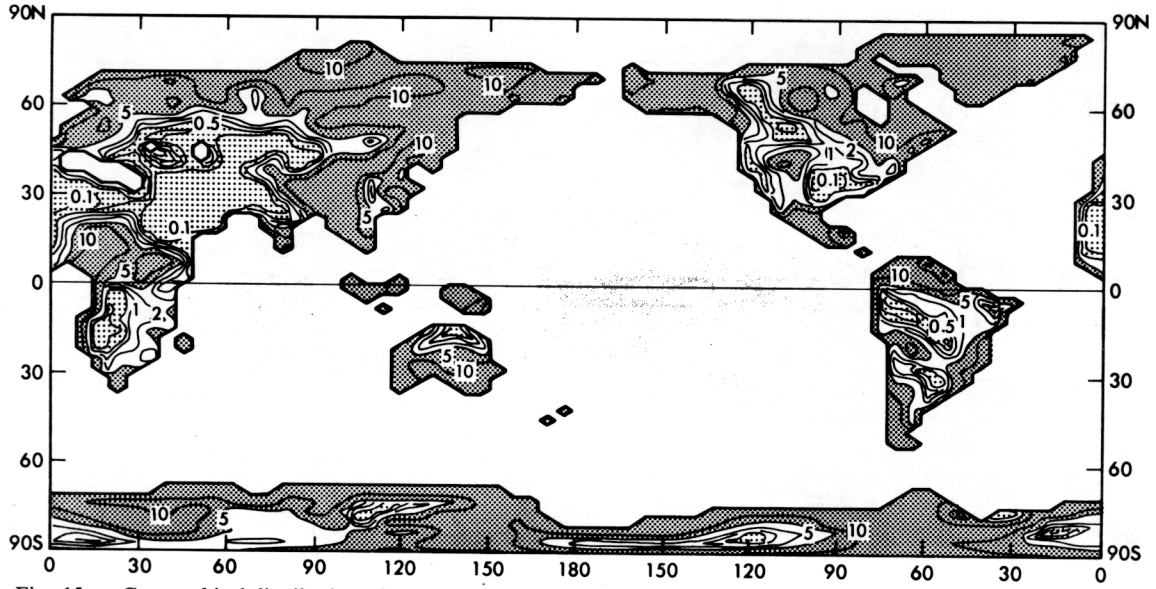

Fig. 15*a*. Geographical distribution of water accumulation in the soil (in cm) computed from the experiment with zonal cloud cover.

nificant, particularly in Africa, southeast and east Asia, and North and South America.

Figure 17 shows the zonally averaged distribution of the signal to noise ratio for the differences of surface pressure (GCL-ZCL). Because the autocorrelation function for pressure decreases at a slower rate than for precipitation, the number of independent states is also less when a time series of the same length is considered. This means that the rms error in the determination of the mean surface pressure will be larger, particularly in the middle latitudes, where the pressure variations are of considerable magnitude. Since the estimation of the significance level for surface pressure was performed from a sampling of the same length, we feel that it is more expedient to show the signal to noise ratio for zonally averaged values. The ratio illustrated in Figure 17 was first computed for the grid points and then averaged along the various latitude circles and slightly smoothed. The autocorrelation function was set to zero after 30 days.

The decrease of mean zonal surface pressure over the continents of the northern hemisphere and its increase over the oceans of the southern hemisphere appear to also be significant.

10. CONCLUSIONS

Two interrelated problems have been discussed in the present study: a computation of a three-dimensional distribution of cloud cover over the globe and an estimation of the effect of this geographical cloud distribution on the model climate.

A method is proposed for the computation of high, middle, and low cloud cover by using the climatic data on total cloud cover and longwave radiation flux at the top of the atmosphere as well as temperature and humidity. The computed vertical extension of the clouds is in fair agreement with the main large-scale features of the general atmospheric circulation: the existence of larger upper cloudiness in the zones of intertropical convergence and baroclinic instability in both

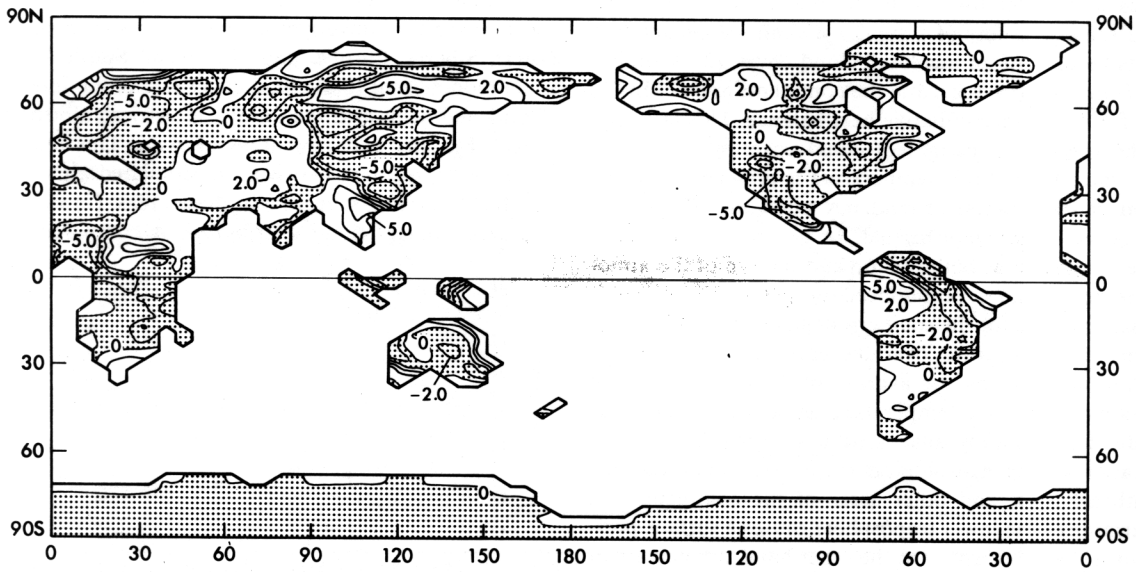

Fig. 15*b*. Geographical distribution of the difference of water accumulated in the soil (in cm) computed from the experiments with zonal and geographical cloud cover (GCL-ZCL).

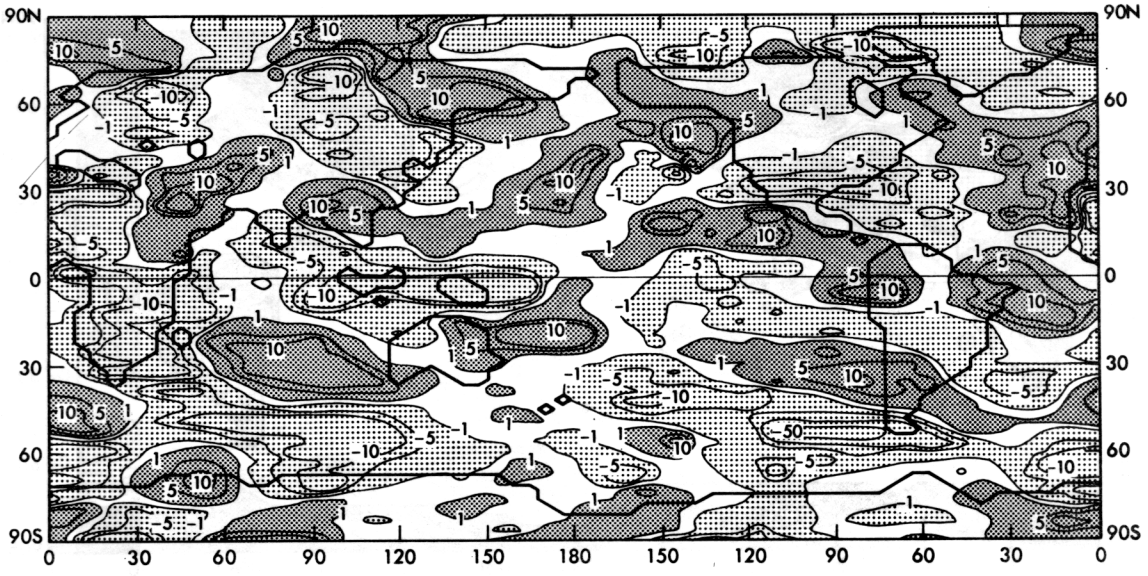

Fig. 16. Geographical distribution of the signal-to-noise ratio for precipitation rate computed from the difference between the GCL and ZCL experiments.

hemispheres and dominance of low cloudiness over relatively cold oceanic waters. The derived vertical structure of the clouds qualitatively also agrees with available observations on the fr quency distribution of dominant types of clouds, in particular, stratiform and cumulus clouds. However, some underestimation of the low cloud cover is revealed over some areas having a large amount of high clouds. This is likely connected with the assumption adopted on the randomness of the cloud distribution at different levels, which, in fact, does not apply in the areas where well organized convection occurs.

A comparison of the numerical experiments performed with an atmospheric general circulation model for July, in which two types of cloud parameterizations are used (i.e., geographical and zonally averaged cloud distributions) has shown that (1) incorporation of a geographical cloud distribution in the model produces marked changes in the net radiation flux at the top of the atmosphere as compared to the ZCL experiment. An analysis of this distribution indicates that a net heat gain takes place over the continents due to less cloudiness there and some heat loss of a similar magnitude occurs over the oceans because of an increased cloud cover. (2) A similar pattern of change, with regard to the continents and oceans, is observed for the surface radiative heat balance. This is, again, due to the respective changes of cloud cover stated above. However, since the oceanic temperature is prescribed, the effect of this surface radiative tendency upon the atmosphere over the oceans is severely limited. In general, the radiative difference tendencies at both the top and bottom of the atmosphere are much more pronounced in the northern hemisphere than they are for the southern hemisphere. (3) Because of the smaller cloud cover over the continents, the surface temperature increases on the average of 2°–4°. However, in some regions the surface temperature decreases by the same magnitude, due to mainly total cloud cover growth and some intensification of the hydrological cycle over equatorial Africa, southeast Asia, and other areas of the continents. (4) Some warming of the lower troposphere causes a surface pressure fall over the continents. On the other hand, an increase of surface pressure is observed over the oceans, particularly in the southern hemisphere. The pressure changes (equal to ±12 mbar) are mostly observed in the middle latitudes of both hemispheres. A tendency toward the formation of a cyclonic circulation is found over the areas with a maximum pressure fall and an anticyclonic circulation is formed over the areas of its maximum rise. (5) The prescribed changes of cloudiness do not have a direct influence on the changes of the precipitation rate since the cloud distribution is not directly related to the precipitation distribution. Instead, they act through other mechanisms of a thermal and dynamical nature: changes in heat and horizontal moisture transport due to the development of a horizontally thermal heterogeneity; development of an unstable condition in moist air due to warming of the lower troposphere; increase of evaporation from the warmer surface, etc. The indirect effect of the geographical cloud variation on the precipitation rate is different for various regions of the globe. Unlike the pressure variation, the largest precipitation rate changes (equal to ±1.0 cm/day) are observed in the tropics in the GCL experiment as compared to the ZCL experiment. A considerable precipitation variation occurs in the intertropical convergence zone, the Asian monsoon area, eastern Siberia, Europe, and North and South America. (6) Some reduction of total cloud cover favors the intensification of arid and semi-arid conditions in Africa, North America, eastern Europe, and vast areas of Asia. This tendency improves the agreement between the simulated atmosphere and the observed climatic regime in these areas. (7) Incorporation of a geographical cloud distribution as compared to zonally

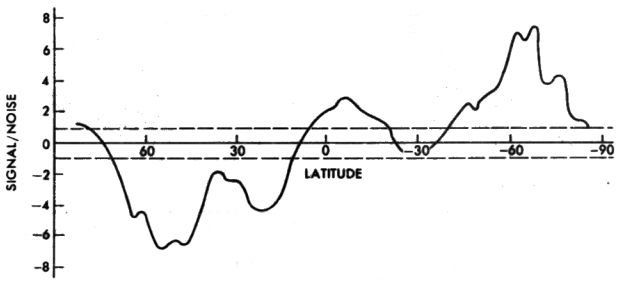

Fig. 17. The zonally averaged distribution of signal-to-noise ratio for sea-surface pressure difference between the GCL and ZCL experiments.

averaged clouds produces some substantial changes in the precipitation rate and surface pressure over some areas of the globe. The estimates of the signal to noise ratio for these two variables have shown that they are statistically significant for many regions. (8) The analysis of the variation of the thermal regime and hydrological cycle of the atmosphere obtained from the model simulation with a different parameterization scheme of cloud distribution has shown that development of more advanced schemes of cloud parameterization will allow an improvement of the simulation capability of the present general circulation models.

APPENDIX: DETERMINATION OF VERTICAL CLOUD DISTRIBUTION

Preliminary Results

Cloud data collected from surface networks and meteorological satellites have been published by *MacDonald* [1938], *London* [1957], *Miller* [1971], *Schutz and Gates* [1971, 1972], *Van Loon et al.* [1972], *Berlyand and Strokina* [1974], *Avaste et al.* [1979], and others. However, climatic data on the vertical extent of clouds are very poor and available, if any, only for highly limited areas of the globe. By using data on the frequency distributions of different types of clouds, *London* [1957] derived zonal distributions of various cloud types for the four seasons. At present, it seems to be the only readily available global data set that contains information on both the vertical extent of different cloud types and their amount. An extensive three-dimensional nephanalysis compiled by the Environmental Technical Applications Center, a branch of the U.S. Air Force, exists, but it is not complete for the entire globe or in a form suitable for this current study.

Improvement of satellite techniques has promoted the development of quantitative methods for the determination of total cloud cover, cloud heights, and other cloud parameters from measurements of outgoing radiation at the water vapor window channel and cloud brightness in the visible range. A thorough review of the relevant studies can be found in two books by *Kondratyev and Timofeev* [1970, 1978]. It is important to note that available data and proposed techniques are not appropriate for the problem discussed in the current paper because they cannot provide vertical distributions of cloud amount over the globe which would be suitable for inclusion in the atmospheric models.

Method for Cloud Determination

The derivation of the vertical cloud distribution is based on an estimation of the thermal differences between the clouds located at a limited number of prescribed levels under the assumption that the total cloud cover, thermal state of the atmospheric column, and distribution of water vapor and other absorbing substances is known.

Let us consider an atmospheric column of unit area extending from the earth's surface to the top of the atmosphere. Suppose that there are three layers of fractional clouds located at different heights so that the total cloud amount N observed from the top of the atmosphere is

$$\sum_{k=1}^{3} N_K = \tilde{N} \tag{1}$$

N_K is a portion of the unit area covered by clouds at the Kth level that can be seen from the top of the atmosphere. At $\tilde{N} = 1.0$ the whole column is completely covered by clouds.

In the case of cloud opacity, the total flux of terrestrial radiation $\tilde{R}$ that reaches the top of the atmosphere consists of the parts that represent the emissions coming from the visible cloud surfaces, the earth's surface, and from the cloudless layers of the atmosphere confined between the radiating surfaces and the top of the atmosphere

$$\sum_{k=0}^{3} N_K R_K = \tilde{R} \tag{2}$$

R_K is the portion of the flux being integrated over the long-wave energy spectrum that reaches the top of the atmosphere from the Kth cloud surface. $N_0 = 1 - \tilde{N}$ is the part of a unit area without clouds, and R_0 is the flux that comes from the land surface.

Let us suppose the following cases.

1. Clouds may exist at not more than three heights of the atmosphere, (high, middle, and low clouds).

2. The heights of the cloud tops are known. The middle and low cloud tops are at the 700 and 925 mbar surfaces, respectively. The high clouds are located at 500 mbar from the pole to about 48° latitude in both hemispheres, then their height increases up to 300 mbar toward the equator [*Feigelson,* 1970; *London,* 1957].

3. The distribution of clouds at each level is random, so that the area of their overlapping is equal to the product of their amounts. The clouds that can be observed from the top of the atmosphere are

$$\begin{aligned} N_1 &= n_1 \\ N_2 &= (1 - n_1)\, n_2 \\ N_3 &= (1 - n_1)\,(1 - n_2) n_3 \end{aligned} \tag{3}$$

4. The clouds radiate as black bodies at the temperature of their surfaces; the middle and low clouds are opaque for long-wave radiation, high clouds are opaque at 90%. The black body assumption is used for high clouds, in addition to the middle and low clouds, to obtain a realistic energy balance at the top of the model atmosphere for the radiative computation.

5. Nonlinear effects due to the use of mean values for atmospheric variables in the radiation computation are negligible [*Budyko,* 1974].

The equations (1) and (2) contain three unknowns N_K (K = 1, 2, 3). An equation similar to (2) but describing the transfer of reflected solar radiation could also be used, and it requires some additional assumptions on cloud properties. However, because the differences between reflected solar fluxes coming from various cloud heights and their overlapping combinations turn out to be marginal to the accurate determination of the total reflected flux, the solution of the equations becomes unstable in some cases. Therefore, the assumption is made that the amount of middle and low clouds is proportional to the corresponding relative humidities at the appropriate levels of the atmosphere. Such a relation is similar to empirically defined linear formulae which are often used for cloud prediction in general circulation models of the atmosphere [*Gates and Schlesinger,* 1977; *Washington and Williamson,* 1977; and others].

Thus it is assumed that

$$\frac{n_2}{n_3} = \frac{h_2}{h_3} \tag{4}$$

hereinafter n_K ($k = 1, 2, 3$) is fractional cloud cover (amount) for high, middle, and low clouds, respectively; h_2 and h_3 are relative humidities at the levels of the atmosphere where middle and low clouds are located.

Taking into account the above assumptions, (2) and (4) may be written in the form

$$\sum_{k=1}^{3} \alpha_K (R_K - R_0) N_K = \tilde{R} - R_0 - (1 - \alpha_1)$$

$$[(R_2 - R_0) n_1 n_2 + (R_3 - R_0)(1 - n_2) n_1 n_3] \quad (5)$$

$$(1 - n_2) \frac{h_3}{h_2} N_2 - N_3 = 0 \quad (6)$$

It follows from the assumption 4 that $\alpha_1 = 0.9$, $\alpha_2 = \alpha_3 = 1$.

The set of equations (1), (5), and (6) may be solved by using an iteration procedure if R_K, $\tilde{R}$, and $\tilde{N}$ are known.

The solution of the equations is not unique in the case of the lapse rate being close to isothermal (for example, a winter condition over continents). From a physical standpoint this implies that owing to small or zero flux differences between different cloud heights it is impossible to identify the vertical cloud structure. However, available cloud statistics for the northern hemisphere show that in such specific cases only stratiform low clouds near the top of the boundary layer are formed [*Dubrovina,* 1975]. Therefore, if the lapse rate in the low troposphere exceeds a prescribed value, the equations (1), (5), and (6) are not used, and the low cloudiness is assumed to be equal to the total cloud amount.

Since the atmospheric parameters needed for the cloud computation are taken from different data sources, they might be inconsistent among themselves in some cases. As a result of this, one can obtain $n_K < 0$ instead of a zero cloud amount at certain heights. Therefore, a procedure for the determination of cloud cover includes a number of consecutive steps. First, the cloud amount is estimated at all three heights by solving equations (1), (5), and (6). The solution must satisfy the following condition

$$0 < N_K < 1 \qquad (K = 1, 2, 3)$$

If $N_K < 0$ for one of the three heights, the cloud cover is then recomputed only for the other two adjacent heights, and assumption 4 is not used in this case. If $N_K < 0$ at one of the two remaining heights, the clouds cannot exist there and it is assumed that they are formed at one height only. Thus, the total cloud cover $\tilde{N}$ is always retained in the column under consideration.

The global three layer cloud distribution is derived for July. The following data sets are used:

1. Monthly mean distribution of total cloud amount over the globe obtained by *Berlyand and Strokina* [1974]. In the belt of 60°–90°S the total clouds were taken from *Van Loon et al.* [1972]. The compiled cloud distribution is given in Figure 3.

2. Monthly means of air temperature and dew point temperature for standard levels of the atmosphere at grid points of 5° × 5° from compilations by *Crutcher and Meserve* [1970] and by *Jenne et al.* [1974].

3. Monthly mean outgoing terrestrial radiation at the top of the atmosphere available at a grid resolution of 10° × 10°. The data were taken from the summary for components of the radiation balance received from satellite measurements during 1964–1970 [*Vonder Haar and Ellis,* 1974].

Temperature and water vapor vertical distributions are prescribed at 13 levels of the model atmosphere. Since the latter is available only up to the 500-mbar surface, the appropriate values for higher levels were obtained by means of extrapolation from lower levels. All data are adjusted to the horizontal resolution of 5° × 5°. The fluxes of R_K were computed from the radiation code developed for the GFDL atmospheric model [*Manabe and Wetherald,* 1967]. The water vapor distribution was estimated from dew-point temperature data. The mixing ratio of carbon dioxide was taken as 0.456×10^{-3} g/kg, and the ozone distribution was prescribed as a function of season, latitude, and height.

Results

Figure 1 illustrates the zonal distribution of computed and observed high, middle, and low clouds. The computation was performed by using zonally averaged terrestrial radiative fluxes, total cloud cover, temperature, and humidity for July. It can be seen that the computed high and low cloud amounts are in fair agreement with the observation in the northern hemisphere. However, some discrepancy can be observed in the southern hemisphere, particularly for high clouds at the latitudinal belt of 30°–60°S. The better agreement of clouds with observation in the northern hemisphere as compared with that in the southern hemisphere apparently results from the quality of available climatic data used in the study. This and other problems relating to the assessment of sensitivity of computed clouds to the assumptions used and uncertainties in the determination of total cloud cover and radiation are thoroughly discussed elsewhere [*Meleshko,* 1980].

Figure 2 shows the geographical distribution of the computed high, middle, and low cloud cover. The following main features of the vertical distribution of computed cloudiness agree with the position of some well-known large-scale patterns of the atmospheric circulation.

1. Large amounts of high clouds in the middle latitudes of both hemispheres which are associated with the positions of the zones of baroclinic instability.

2. Well-pronounced maximum of high cloud cover over southeast Asia and India that is attributed to the development of the southwest and southeast monsoon circulation during the summer.

3. Areas of increased high clouds in the vicinity of the equator that are associated with the position of the inter-tropical convergence zone.

4. Low clouds over considerable areas of the oceans in the northern hemisphere. Two such areas are in the northeast Pacific and off the west coast of South America over the cold oceanic waters.

Besides the indicated features, which agree well with available qualitative cloud data, some features are also revealed that seem to result from assumptions used in the computational scheme as well as some deficiencies in the available climatic data. One can notice the lack of maxima in low cloud cover over southeast Asia, the equatorial belt of the Pacific, and the South Pacific around the Antarctic coast where the high cloud maxima are computed. One of the basic assumptions suggests that the cloud distribution at adjacent levels is random with respect to one another, and this is apparently valid for regions where stratiform clouds prevail but not for convective clouds with considerable vertical development. As

a consequence of this, the low cloud cover suffers from some underestimation over the areas with a large amount of high clouds.

With regard to the intertropical convergence zone, there are two factors that may contribute to cloud underestimation there. The observed total cloud cover does not show a continuous maximum zone over the equatorial Pacific. This shortcoming can affect the computed low clouds. Moreover, the radiation data, presented at a relatively coarse grid (10° × 10°), appears to be inadequate to resolve the cloud patterns in certain areas, where the intertropical convergence forms a rather narrow zone.

In conclusion, it can be pointed out that except for certain regions where deficiencies are revealed in the low cloud cover the computed vertical extent of the clouds is in fair agreement with the main large-scale patterns of the general circulation of the atmosphere during July.

Acknowledgments. In accordance with the Soviet-American agreement on scientific collaboration in connection with protection of the environment (Working Group 8), V. P. Meleshko has visited the Geophysical Fluid Dynamics Laboratory, NOAA, Princeton University, to study sensitivity and stability of climate to external forcing. The present study has been carried out during his 6-month stay at GFDL in 1978 jointly with R. T. Wetherald.

We would like to express our gratitude to J. Smagorinsky for making this international joint research effort possible. We are particularly grateful to S. Manabe for making available to us the most recent version of the GFDL climate general circulation model and coordinating its usage, as well as making many valuable suggestions throughout this study. The authors wish to thank D. Daniel for his effective management of the model integrations and L. Dimmick for valuable assistance in the computer analysis of the results. Finally, we would like to acknowledge the prompt and efficient assistance of Joyce Kennedy, Philip Tunison, John Connor, Michael Zadworny, and William Ellis for the preparation of the manuscript and figures.

REFERENCES

Avaste, O. A., G. G. Campbell, S. K. Cox, D. DeMasters, O. U. Karner, K. S. Shifrin, E. A. Smith, E. J. Steiner, and T. H. Vonder Haar, On the estimation of cloud-amount distribution above the world oceans, *Atmos. Sci. Pap. 309,* Dep. of Atmos. Sci., Colorado State Univ., Fort Collins, Colo., 1979.

Berlyand, T. G., and L. A. Strokina, Cloudiness regime over the globe, *Phys. Climatol., MGO Trudy, 338,* 3–20, 1974.

Bourke, W., A multi-level model, I, Formulation and hemispheric integrations, *Mon. Weather Rev., 102,* 688–701, 1974.

Bourke, W., B. McAvaney, K. Puri, and R. Thurling, Global modeling of atmospheric flow by spectral methods, in *Methods in Computational Physics,* pp. 267–324, 1977.

Budyko, M. I., *Climate and Life, Int. Geophys. Ser.,* vol. 18, edited by D. H. Miller, Academic, New York, 1974.

Cess, R. D., Climate change: An appraisal of atmospheric feedback mechanisms employing zonal climatology, *J. Atmos. Sci., 33,* 1831–1843, 1976.

Cess, R. D., and V. Ramanathan, Averaging of infrared cloud opacities for climate modelling, *J. Atmos. Sci., 35,* 919–922, 1978.

Charney, J., W. J. Quirk, S.-H. Chow, and J. Kornfield, A comparative study of effects of albedo change on drought in semi-arid regions, *J. Atmos. Sci., 34,* 1366–1365, 1977.

Crutcher, H. L., and J. M. Meserve, Selected level heights, temperature and dew points for the northern hemisphere, *NAVAIR 50-IC-52,* U.S. Nav. Weather Serv., Washington, D. C., 1970.

Dubrovina, L. S., Statistical characteristics of spatial and microphysical structure of clouds, in *Aviation-Climatic Atlas-Handbook of the USSR,* vol. 1, 2, issue 3, Gidrometeoizdat, Moscow, 1975.

Eliassen, E., B. Machenhauer, and E. Rasmussen, On a numerical method for integration of the hydrodynamical equations with a spectral representation of the horizontal fields, *Rep. 2,* Inst. for Teoretisk Meteorol., Köbenhavns Univ., Denmark.

Ellis, J. S., Cloudiness, the planetary radiation budget and climate, Ph.D. thesis, Colorado State Univ., Fort Collins, 1978.

Ellis, J. S., and T. H. Vonder Haar, Zonal average earth radiation budget measurements from satellites for climate studies, *Atmos. Sci. Pap. 240,* Colorado State Univ., Fort Collins, 1976.

Feigelson, E. M., Radiative heat exchange in the clouds, *Gidrometeoizdat,* Leningrad, 1970.

Gates, W. L., and M. E. Schlesinger, Numerical simulation of the January and July global climate with a two-level atmospheric model, *J. Atmos. Sci., 34,* 36–76, 1977.

Gordon, C. T., and W. F. Stern, The GFDL global spectral model, submitted to *Mon. Weather Rev.,* 1981.

Holloway, J. L., Jr., and S. Manabe, Simulation of climate by a global general circulation model, *Mon. Weather Rev., 99,* 335–370, 1971.

Hoskins, J. J., and A. J. Simmons, A multi-layer spectral model and the semi-explicit method, *Q. J. R. Meteorol. Soc., 104,* 91–102, 1975.

Jenne, R. L., H. L. Crutcher, H. van Loon, and J. J. Taljaard, A selected climatology of the southern hemisphere: Computer methods and data availability, *Tech. Note NCAR-TN/STR-92,* Nat. Center Atmos. Res., Boulder, Colo., 1974.

Kondratiev, K. Ya., and Yu. M. Timofeev, The thermal sounding of the atmosphere from satellites, *Gidrometeoizdat,* Leningrad, 1970.

Kondratiev, K. Ya., and Yu. M. Timofeev, The thermal sounding of the atmosphere from the space, *Gidrometeoizdat,* Leningrad, 1978.

Leith, C. E., The standard error of time average estimates of climatic means, *J. Appl. Meteorol., 12,* 1066–1069, 1973.

London, J. A., Study of the atmospheric heat balance, *final report,* Coll. of Eng., New York Univ., New York, 1957.

Manabe, S., and R. F. Strickler, Thermal equilibrium of the atmosphere with a convective adjustment, *J. Atmos Sci., 21,* 361–385, 1964.

Manabe, S., and R. T. Wetherald, Thermal equilibrium of the atmosphere with a given distribution of relative humidity, *J. Atmos. Sci., 24,* 241–259, 1967.

Manabe, S., D. G. Hahn, and J. L. Holloway, Jr., Climate simulation with GFDL spectral models of the atmosphere: Effect of spectral truncation, *GARP Publ. Ser. 22,* World Meteorol. Organ., Geneva, 1979.

McDonald, W. F. (Ed.), *Atlas of Climatic Charts of the Oceans,* U.S. Government Printing Office, Washington, D. C., 1938.

Meleshko, V. P., Computation of global distribution of three-layer large-scale cloudiness, *Meteorol. Gidrologia, 9,* 12–23, 1980.

Miller, B. D., Global Atlas of Relative Cloud Cover 1967-1970, U.S. Dep. of Commerce, Washington, D. C., 1971.

Musaelyan, S. A., On parameterization of solar energy exchange in the ocean-atmosphere system and long-range forecasting, *Meteorol. Gidrologia, 10,* 9–19, 1974.

Musaelyan, S. A., On the nature of some long-term atmospheric processes, *Gidrometeoizdat,* Leningrad, 1978.

Orszag, S. A., Transform method for the calculation of vector-coupled sums: Application to the spectral form of the vorticity equation, *J. Atmos. Sci., 27,* 890–895, 1970.

Schneider, S. H., Cloudiness as a global climatic feedback mechanism: the effects on the radiation balance and surface temperature of variation in cloudiness, *J. Atmos. Sci., 29,* 1413–1422, 1972.

Shutz, C., and W. L. Gates, Global climatic data for surface, 800 mb, 400 mb: July, R-1029-ARPA, the RAND Corp., Santa Monica, Calif., 1971.

Schutz, C., and W. L. Gates, Global climatic data for surface, 800 mb, 400 mb: January, *R-915-ARPA,* The RAND Corp., Santa Monica, Calif., 1972.

Somerville, R. C. J., P. H. Stone, M. Halem, J. E. Hansen, J. S. Hogan, L. M. Druyan, G. Russell, A. A. Lacis, W. J. Quirk, and J. Tenenbaum, The GISS model of the global atmosphere, *J. Atmos. Sci., 31,* 84–117, 1974.

Van Loon, H., J. J. Taljaard, T. Sasamori, J. London, D. V. Hoyt, K. Labitzke, and C. W. Newton, *Meteorology of the Southern Hemisphere, Meteorol. Monogr.,* vol. 13, American Meteorological Society, Boston, Mass., 1972.

Vonder Haar, T. H., and J. S. Ellis, Atlas of radiation budget measurements from satellites (1962-1970), *Atmos. Sci. Pap. 231,* Colorado State Univ., Fort Collins, Colo., 1974.

Washington, W. M., and D. L. Williamson, A description of the

NCAR global circulation model, in *Methods in Computational Physics,* vol. 17, Academic, New York, 1977.

Webster, P. J., and L. C. Chou, Seasonal structure of a simple monsoon system, *J. Atmos. Sci., 37,* 354–382, 1980.

Wetherald, R. T., and S. Manabe, The effects of changing the solar constant on the climate of a general circulation model, *J. Atmos. Sci., 32,* 2044–2059, 1975.

Wetherald, R. T., and S. Manabe, Cloud cover and climate sensitivity, *J. Atmos. Sci., 37,* 1485–1500, 1980.

(Received June 16, 1980;
revised August 10, 1981;
accepted August 11, 1981.)